

Ponding Analysis with Green-and-Ampt Infiltration

Hugo A. Loáiciga¹ and Allison Huang²

Abstract: The ponding of water over level terrain caused by storms of arbitrary temporal intensity is quantified by solving water-balance differential equations involving cumulative rainfall, infiltration, the depth of ponded water, and evaporation of ponded water. Infiltration is quantified using an extended Green-and-Ampt formulation in which the depth of ponded water influences the infiltration rate. A numerical algorithm for calculating the infiltration and ponding hydrographs is developed and applied in this work. The maximum depth of ponded water and the duration of ponding are among the variables that can be calculated with the method presented in this paper. These variables are useful in basin irrigation and in wetland wetting and restoration.

DOI: 10.1061/(ASCE)1084-0699(2007)12:1(109)

CE Database subject headings: Infiltration; Rainfall; Soil water; Evaporation; Numerical analysis.

Introduction

This note presents a methodology to quantify rainfall-driven flooding of low-permeability soils in which there is lateral containment of ponded water and negligible lateral drainage. Examples of this type of hydrologic environments are vernal pools and irrigation basins (see Loáiciga and Huang 2005). Infiltration is described in this work with the widely used Green-and-Ampt infiltration model (Green and Ampt 1911; Philip 1993). This paper's contribution is to provide a general formulation and method of solution of the water-balance equations governing cumulative infiltration and ponding caused by intense rainfall of arbitrary temporal distribution. The calculation of the hydrograph of ponded water yields the duration of ponding and the maximum depth of ponded water. These two variables are useful in basin irrigation and wetland wetting and restoration. Two examples illustrate the application of the methods advanced in this work.

A General Equation for the Time at Which Ponding Begins (t_p)

There is a finite interval that precedes the initiation of ponding. Rainfall storms typically start with low intensity, which increases over time, and then recedes. Fig. 1 illustrates the hyetograph for the Type I, 24-h duration, 100-year storm used by the U.S. Agricultural Research Service [which encompasses what used to be

called the Soil Conservation Service (SCS)]. The SCS Type I storm—typical of southern California regions—will be used in the examples presented later in this paper. As rainfall intensity increases it eventually surpasses the capacity of a soil to infiltrate all the incoming water. The Green-and-Ampt infiltration model uses Darcy's law to calculate the actual infiltration rate (f) in a vertical, homogeneous, soil column. The soil features an initial moisture deficit (equal to its porosity minus the initial volumetric water content, $n-v_0$), a constant soil-water tension at the downward-advancing saturation front (ψ_f , where $\psi_f > 0$, a soil property), and a saturated hydraulic conductivity (K_{sat}). A saturation front at a depth z_f (measured vertically from the ground surface, $z_f < 0$) implies a cumulative infiltration $F(t) = |z_f(t)|(n-v_0)$. The rainfall rate (w) equals the infiltration rate (f) before ponding begins. Therefore, the cumulative infiltration equals cumulative rainfall, $F(t) = W(t)$, in which $W(t)$ = cumulative rainfall from time zero to time t before ponding begins. This is captured by the following water-balance equation for the time of ponding initiation, t_p :

$$W(t_p) = |z_f(t_p)|(n-v_0) \quad (1)$$

Writing Darcy's law between the ground surface (i.e., at $z=0$, where the hydraulic head is zero) and $z_f(t_p)$ [where the hydraulic head equals $z_f(t_p) - \psi_f$], setting the magnitude of the Darcian

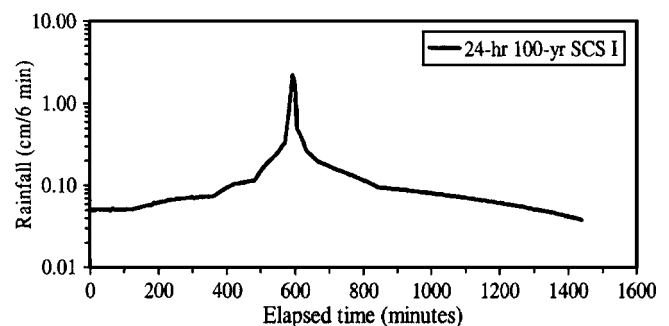


Fig. 1. Hyetograph of the SCS Type I, 24-h, 100-year storm used in the example simulations. Total rainfall depth equals 29.2 cm.

¹Professor, Dept. of Geography, UCSB, Santa Barbara, CA 93106. E-mail: hugo@geog.ucsb.edu

²Research Assistant, Bren School of Environmental Science and Management, UCSB, Santa Barbara, CA 93106.

Note. Discussion open until June 1, 2007. Separate discussions must be submitted for individual papers. To extend the closing date by one month, a written request must be filed with the ASCE Managing Editor. The manuscript for this technical note was submitted for review and possible publication on November 27, 2002; approved on May 19, 2006. This technical note is part of the *Journal of Hydrologic Engineering*, Vol. 12, No. 1, January 1, 2007. ©ASCE, ISSN 1084-0699/2007/1-109-112/\$25.00.

flux—which equals the infiltration rate—equal to the rainfall rate at time t_p [i.e., $w(t_p)$], and solving for the wetting-front depth produces the following result:

$$|z_f(t_p)| = \frac{K_{sat}\psi_f}{w(t_p) - K_{sat}} \quad (2)$$

with $w(t_p) > K_{sat}$ required for ponding to occur. Combining Eqs. (1) and (2) yields the equation for the time to ponding t_p

$$W(t_p) = \frac{K_{sat}\psi_f}{w(t_p) - K_{sat}}(n - v_0) \quad (3)$$

The rainfall function evaluated at time t_p , $w(t_p)$, is known. The solution of Eq. (3) for t_p requires numerical approximation for variable rainfall input.

Water-Balance Equations for Infiltration and Ponding during Rainfall

In the interval following the onset of ponding and until the end of rainfall (at time t_R), the cumulative rainfall [$W(t)$, a known input] equals the sum of cumulative infiltration [$F(t)$] plus cumulative ponding [$Y(t)$]. The infiltration rate, $f(t) = F'(t)$, is expressed via Darcy's law as follows:

$$F' \equiv f = \frac{K_{sat}[Y - (z_f - \psi_f)]}{|z_f|} \quad (4)$$

which is expanded to produce the following ODE for the cumulative infiltration $F(t)$ in the interval $t_p \leq t \leq t_R$:

$$FF' - vF - c(W(t) + \psi_f) = 0, \quad t_p \leq t \leq t_R \quad (5)$$

whose initial condition is $F(t_p) = W(t_p)$; and in which $v = K_{sat}(1 - (n - v_0))$, $c = K_{sat}(n - v_0)$. Eq. (5) governs the evolution of infiltration from the onset of ponding until the end of rain. Having $F(t)$, the ponding depth is calculated from $Y(t) = W(t) - F(t)$. Evaporation is nil during rainfall. The magnitude of the depth of the saturation front is given by $|z_f(t)| = F(t)/(n - v_0)$. The solution of Eq. (5) can be obtained accurately with numerical solvers of the Runge-Kutta type (see Loáiciga and Huang 2005), as shown in the section entitled "Results."

The cumulative rainfall $W(t)$ is rarely expressible in terms of elementary functions. Rather, it must be constructed from hyetographs such as that shown in Fig. 1 for the 24-h, 100-year, Type I SCS rainfall. Rainfall intensities are expressed as constant values over consecutive 6-min intervals in the hyetograph of Fig. 1. In this type of situation, Eq. (5) is solved sequentially over each constant-rainfall interval using the beginning-of-interval cumulative infiltration as the initial condition and the specified rainfall from the hyetograph corresponding to the interval in question. The end-of-interval cumulative infiltration so obtained becomes the initial condition for the next interval, and so on, until the end of rainfall. Notice, however, that the ODE in each constant-rainfall interval now takes a form simpler than that given in Eq. (5). It is advantageous then to rewrite the ODE as follows in the j th constant-rainfall interval:

$$FF' - vF - cw_j(t + d_j) = 0 \quad (6)$$

in which the v and c coefficients were given after Eq. (5) and $w_j = (\text{constant})$ rainfall rate that applies during the j th interval of simulation. The d_j coefficient in Eq. (6) is given by $d_j = (\psi_f/w_j) + (W(t_j)/w_j) - t_j$, in which t_j and $W(t_j)$ denote the starting time of the j th interval and the cumulative rainfall at time t_j , respectively. The initial condition of Eq. (6) is $F(t_j)$, which is equal to the calculated cumulative infiltration at the end of the previous constant-rainfall interval.

Water-Balance Equations for Infiltration and Ponding after Rainfall

It is assumed in this section that there is ponding extant at a the end of rainfall. Otherwise, the simulation of infiltration and ponding ends at this time. In the former case, ponding is reduced by infiltration and evaporation (denoted by e_v , a time-dependent rate, in general) after rainfall. Evaporation (a known input function) starts at $t = t_R$, i.e., at the end of rainfall. The water balance equation in the post-rainfall period is $W(t_R) = Y(t) + F(t) + E(t)$, $t > t_R$, in which $E(t)$ = cumulative evaporation, and the cumulative precipitation $W(t_R)$ is constant. Relying on Darcy's law, in a manner analogous to that of the previous section, leads to the following ODE for the cumulative infiltration $F(t)$ in the post-rainfall phase:

$$FF' - vF - c \cdot (W(t_R) + \psi_f - E(t)) = 0 \geq, \quad t_R \quad (7)$$

whose initial condition is $F(t_R)$, equal to the cumulative infiltration at the end of rainfall, and the coefficients c and v are as already stated. The solution of Eq. (7) can be achieved accurately with Runge-Kutta numerical solvers. The ponding depth is calculated as $Y(t) = W(t_R) - F(t) - E(t)$, once $F(t)$ is calculated.

Evaporation rates are commonly specified as constant values over consecutive intervals. In this case Eq. (7) is solved sequentially over each constant-evaporation interval using the beginning-of-interval cumulative infiltration as the initial condition and the specified evaporation rate in the interval in question. The end-of-interval cumulative infiltration so obtained becomes the initial condition for the next interval, and so on, until the depth of ponded water vanishes under the combined action of evaporation and infiltration. The ODE in each constant-evaporation interval now takes the following simpler form in the j th constant-evaporation interval:

$$FF' - vF + ce_{vj}(t - d_{ej}) = 0 \quad (8)$$

in which the v and c coefficients are as stated earlier and $e_{vj} = (\text{constant})$ evaporation rate that applies in the j th interval of simulation. The d_{ej} coefficient in Eq. (8) is given by $d_{ej} = \{[W(t_R) + \psi_f - E(t_j)]/e_{vj}\} + t_j$, in which t_j and $E(t_j)$ denote the starting time of the j th interval and the cumulative evaporation at time t_j , respectively. The initial condition of Eq. (8) is $F(t_j)$, which is equal to the calculated cumulative infiltration at the end of the previous constant-evaporation interval. The extinction time t_F at which ponding vanishes under the combined action of infiltration and evaporation marks the end of simulation.

Results

The calculation of ponding driven by variable rainfall is illustrated using the hyetograph shown in Fig. 1 (total storm depth = 29.2 cm) and two soils with substantially different hydraulic

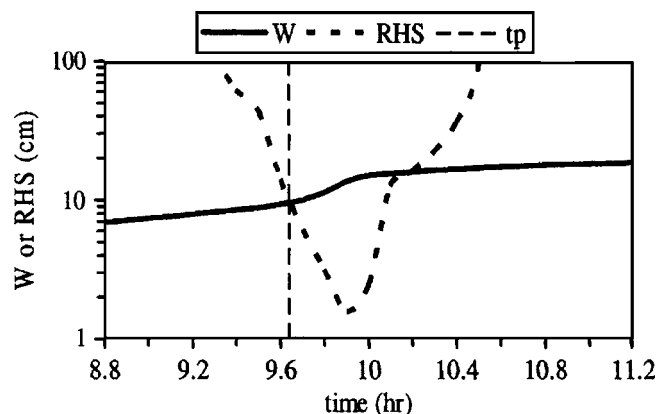


Fig. 2. Graph showing the determination of the time at which ponding begins (t_p) in the silt-loam soil. $t_p=9.64$ h, and is indicated by the vertical dotted line. W and RHS denote cumulative rainfall and the right-hand side of Eq. (3), respectively.

conductivity. The latter choice shall illustrate the important role of hydraulic conductivity (K_{sat}) on infiltration and ponding. The first soil is silt-loam for which porosity (n), K_{sat} , and wetting front-tension (ψ_f) equal 0.485, 2.59 cm/h, and 64.4 cm, respectively. The second soil, a silt-clay, has $n=0.492$, $K_{sat}=0.371$ cm/h, and $\psi_f=43.5$ cm. Notice that the silt-clay's K_{sat} is approximately seven times smaller than that of the silt-loam. The simulations of infiltration (and ponding) used a starting initial (volumetric) water content $v_0=0.30$ in the two soils. It was assumed that the evaporation rate was negligible following rainfall.

Fig. 2 gives a graphical representation of the determination of the time to ponding in the silt-loam soil, for which $t_p=9.64$ h. t_p occurs when the cumulative infiltration equals the right-hand side of Eq. (3) for the first time. Fig. 3 presents similar information for the silt-clay soil, whose $t_p=7.10$ h. Evidently, ponding arises first in the less permeable soil, the silt-clay. Notice that ponding begins only after the rainfall intensity (shown in Fig. 1) rises sharply.

Fig. 4 displays the calculated hydrographs for cumulative infiltration and the depth of ponded water, as well as the cumulative rainfall, in the silt-loam. It can be seen that ponding is short lived, lasting about 2.2 h, from 9.64 to 11.8 h after the start of rainfall. The maximum depth of ponded water, a variable of interest in

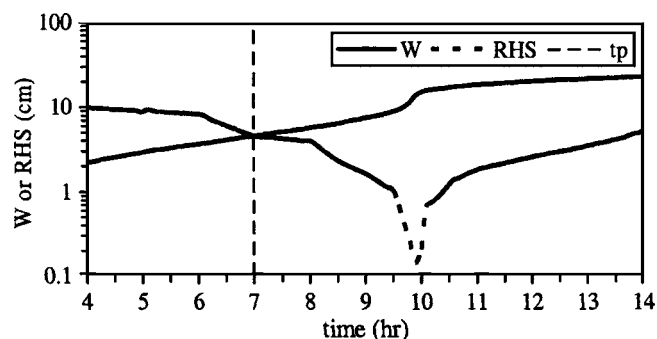


Fig. 3. Graph showing the determination of the time at which ponding begins (t_p) in the silt-clay soil. $t_p=7.10$ h, and is indicated by the vertical dotted line. W and RHS denote cumulative rainfall and the right-hand side of Eq. (3), respectively.

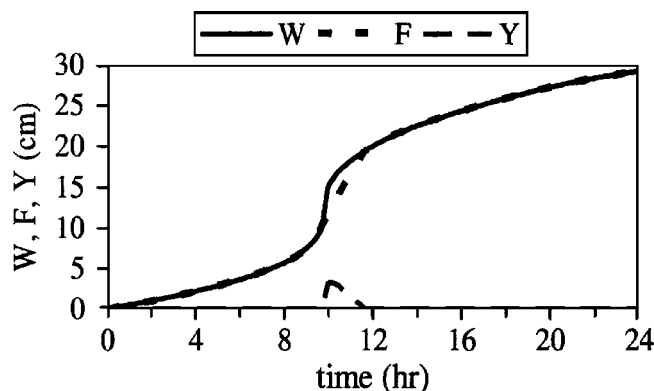


Fig. 4. Hydrographs of cumulative rainfall (W), infiltration (F), and depth of ponded water (Y) in silt-loam soil. The time to ponding is $t_p=9.64$ h. See the text for more details.

basin irrigation and in wetland wetting and restoration, was 3.4 cm, and occurred 10.0 h after the beginning of rainfall.

Calculated hydrographs for cumulative infiltration and ponding (as well as for the cumulative rainfall) in silt-clay are shown in Fig. 5. Ponding lasted 42.9 h, from 7.10 to 50.0 h after the beginning of rainfall, well beyond the end of rainfall at $t=24$ h. The maximum ponding depth was 14.1 cm, and took place 22.0 h after the beginning of rainfall. An interesting feature of the cumulative infiltration hydrograph in Fig. 4 is its nearly linear shape, which is visibly different from the nonlinear, S-shaped, cumulative infiltration in silt-loam depicted in Fig. 4.

The previous results demonstrate the strong influence of hydraulic conductivity and textural properties (reflected in the wetting-front suction ψ_f) on infiltration, and, thus, on the ponding of water over level soils. Such influence is well reflected on the time at which ponding begins, on the duration of ponding, and on the maximum depth of ponded water. These variables are important in the controlled flooding of land, such as in basin irrigation and wetland wetting and restoration. The calculations of infiltration and ponding shown in Figs. 4 and 5 were carried out using a Runge-Kutta ODE solver available in the software MATLAB (The MathWorks, Inc., Natic, Mass.). The iterative scheme embodied by Eq. (6) was implemented using the cited software.

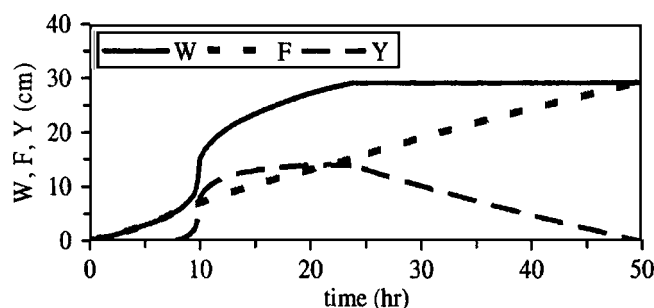


Fig. 5. Hydrographs of cumulative rainfall (W), infiltration (F), and depth of ponded water (Y) in silt-clay soil. The time to ponding is $t_p=7.10$ h. See the text for more details.

Future work in computational infiltration will focus on simulating the depth of water flowing over gently sloping terrain driven by rainfall, and affected by infiltration. This task entails coupling equations of surface flow and infiltration.

Acknowledgments

This research was funded in part by National Science Foundation Grant No. 0114437.

References

- Green, W. H., and Ampt, G. A. (1911). "Studies on soil physics. 1. The flow of air and water through soils." *J. Agric. Sci.*, 4(1), 1–24.
- Loáiciga, H. A., and Huang, A. (2005). "Flooding-cycle analysis in wetlands with negligible overland drainage." *Dynamics and biogeochemistry of river corridors and wetlands*, International Association of Hydrological Sciences (IAHS), Publ. No. 294, Wallingford, U.K., 122–129.
- Philip, J. R. (1993). "Variable-head ponded infiltration under constant or variable rainfall." *Water Resour. Res.*, 29(7), 2155–2165.